Carcinogenesis vol.33 no.11 pp.2208–2219, 2012
doi:10.1093/carcin/bgs213
Advance Access publication July 10, 2012

Proteomic and pathway analyses reveal a network of inflammatory genes associated with differences in skin tumor promotion susceptibility in DBA/2 and C57BL/6 mice

Jianjun Shen[1,*], Erika L.Abel[1], Penny K.Riggs[2], John Repass[6], Sean C.Hensley[1], Lisa J.Schroeder[1], Angelina Temple[1], Alexander Chau[1], S.Alex McClellan[3], Okkyung Rho[3], Kaoru Kiguchi[3], Michael D.Ward[4], O.John Semmes[4], Maria D.Person[3], Joe M.Angel[3] and John DiGiovanni[3,5,*]

[1]Department of Molecular Carcinogenesis, Science Park, The University of Texas, M.D. Anderson Cancer Center, Smithville, TX 78957, USA, [2]Department of Animal Science, College of Agriculture and Life Sciences, Texas A&M University, College Station, TX 77834, USA, [3]Division of Pharmacology and Toxicology, College of Pharmacy, The University of Texas at Austin, TX 78712, USA, [4]The Leroy T. Canoles Cancer Research Center, Eastern Virginia Medical School, Norfolk, VA 23507, USA, [5]Department of Nutritional Sciences, College of Natural Sciences, The University of Texas at Austin, TX 78712, USA and [6]ARQ Genetics, Bastrop, TX 78602, USA

*To whom correspondence should be addressed. John DiGiovanni, The University of Texas Dell Pediatric Research Institute, 1400 Barbara Jordan Blvd., Austin, TX 78723, USA. Tel: +512 495 4726; FAX: +512 495 4947; Email: jdigiovanni@mail.utexas.edu
Jianjun Shen, The University of Texas M.D. Anderson Cancer Center, Department of Molecular Carcinogenesis, Science Park, 1808 Park Road 1C, PO Box 389, Smithville, TX 78957, USA. Tel: +512 237 9558; Fax: +512 237 2475;Email: jianshen@mdanderson.org

Genetic susceptibility to two-stage skin carcinogenesis is known to vary significantly among different stocks and strains of mice. In an effort to identify specific protein changes or altered signaling pathways associated with skin tumor promotion susceptibility, a proteomic approach was used to examine and identify proteins that were differentially expressed in epidermis between promotion-sensitive DBA/2 and promotion-resistant C57BL/6 mice following treatment with 12-O-tetradecanoylphorbol-13-acetate (TPA). We identified 19 differentially expressed proteins of which 5 were the calcium-binding proteins annexin A1, parvalbumin α, S100A8, S100A9, and S100A11. Further analyses revealed that S100A8 and S100A9 protein levels were also similarly differentially upregulated in epidermis of DBA/2 versus C57BL/6 mice following topical treatment with two other skin tumor promoters, okadaic acid and chrysarobin. Pathway analysis of all 19 identified proteins from the present study suggested that these proteins were components of several networks that included inflammation-associated proteins known to be involved in skin tumor promotion (e.g. TNF-α, NFκB). Follow-up studies revealed that Tnf, Nfkb1, Il22, Il1b, Cxcl1, Cxcl2 and Cxcl5 mRNAs were highly expressed in epidermis of DBA/2 compared with C57BL/6 mice at 24 h following treatment with TPA. Furthermore, NFκB (p65) was also highly activated at the same time point (as measured by phosphorylation at ser276) in epidermis of DBA/2 mice compared with C57BL/6 mice. Taken together, the present data suggest that differential expression of genes involved in inflammatory pathways in epidermis may play a key role in genetic differences in susceptibility to skin tumor promotion in DBA/2 and C57BL/6 mice.

Abbreviations: 2-D PAGE, two-dimensional polyacrylamide gel electrophoresis; Chry, chrysarobin; IHC, immunohistochemical; IPA, ingenuity pathway analysis; MS, mass spectrometry; OA, okadaic acid TPA, 12-*O*-tetradecanoylphorbol-13-acetate; MS, mass spectometry; qPCR, quantitative real-time polymerase chain reaction; RIPA, radio-immunoprecipitation assay;IPG, immobilized pH gradient; KO, knockout; MALDI-TOF, matrix-assisted laser desorption/ionization time of flight; 1D, 1-dimentional; SDS, sodium dodecyl sulfate.

Introduction

Genetic susceptibility to two-stage skin carcinogenesis is known to vary dramatically among different stocks and strains of mice (1–5). For example, P/J, C3H, A/J, DBA/2 and SENCAR mice are relatively sensitive to tumor promotion by the phorbol ester, 12-O-tetradecanoylphorbol-13-acetate (TPA), whereas AKR, BALB/c and C57BL/6 mice are relatively resistant (6–8). Our laboratory previously demonstrated that genetic control of susceptibility to skin tumor promotion by TPA in crosses between susceptible DBA/2 and resistant C57BL/6 mice is a multi-genic trait. In those studies, localized regions on mouse chromosomes 1, 2, 9 and 19 were identified that contained potential tumor promotion susceptibility genes (9–11). Other laboratories have also identified additional chromosomal regions associated with skin tumor susceptibility and progression using different genetic crosses (4,5,12–21).

Another approach to identify genes that modify susceptibility to skin tumor promotion is to conduct global gene expression analyses in sensitive and resistant mouse strains after treatment with tumor promoters such as TPA. Recently, altered global gene expression after TPA treatment has been analyzed in mouse epidermis and keratinocytes by microarray and suppression subtractive hybridization (22,23). In general, these studies focused on gene expression in epidermis or cultured keratinocytes from single mouse strains after a single TPA treatment. Recently, we conducted a microarray analysis to compare gene expression profiles from epidermis of DBA/2J and C57BL/6J mice treated with TPA as a means to identify genes that modify promotion susceptibility (24). In this previous study, 44 genes were identified as differentially expressed in epidermal RNA samples between the two strains at 6 h after the last of four TPA treatments. Eleven of these differentially expressed genes were located within regions previously mapped for promotion susceptibility loci (9–11,25). One of these genes, glutathione S-transferase, alpha 4 (*Gsta4*) located on distal Chr 9 was identified as the skin tumor promotion susceptibility gene located at *Psl1.2* (26).

In the present study, we employed the approach of two-dimensional (2-D) gel electrophoresis followed by mass spectrometry (MS) to identify differentially expressed proteins in epidermis between DBA/2 and C57BL/6 mice following treatment with TPA. This approach has been used in recent studies to successfully delineate altered protein expression profiles in epidermal tissue of several different transgenic mouse models (27,28). We anticipated that a proteomics-based approach would complement global gene expression analyses and also provide additional information concerning post-translational modification of expressed proteins. In the current study, 19 distinct proteins were identified as differentially expressed, most with higher expression in the epidermis of DBA/2 mice compared with C57BL/6 mice. These proteins included S100A8, S100A9 and S100A11, as well as two other calcium-binding proteins (parvalbumin α and annexin A1). Elevated expression of S100A8 and S100A9 proteins is a hallmark of several inflammation-associated diseases (such as multiple sclerosis, cystic fibrosis, chronic inflammatory bowel diseases and psoriasis) (29). Differential expression of these two proteins was further confirmed by western blot analyses, immunohistochemical (IHC) analyses and quantitative real-time polymerase chain reaction (qPCR). Ingenuity Pathway Analysis (IPA) revealed these proteins to be part of several networks that included inflammation-associated proteins (i.e. TNF-α, NFκB and IL-22). Further analyses revealed that Tnf, Nfkb1, Il22, Il1b, Cxcl1, Cxcl2 and Cxcl5 mRNAs were significantly upregulated in epidermis of DBA/2 compared with C57BL/6 mice at 24 h following treatment with TPA. Further analyses revealed that NFκB (p65) was activated (phosphorylated at ser276) to a greater extent in epidermis of DBA/2 mice compared with C57BL/6 mice at the same time point. The current data provide new information about possible molecular mechanisms for the differential

susceptibility of DBA/2 and C57BL/6 mice to the tumor-promoting activity of TPA and possibly other skin tumor promoting agents.

Materials and methods

Mice and treatment of mouse skin

Age-matched female C57BL/6 and DBA/2 mice were purchased from The Jackson Laboratory (Bar Harbor, ME). Mice were maintained for at least 2 weeks prior to treatment in the specific pathogen-free Animal Resource Facility at the Science Park-Research Division of the University of Texas M.D. Anderson Cancer Center as described previously (3,7) and approved by the Institutional Animal Care and Use Committee. At 6 weeks of age, the backs of mice were carefully shaved using surgical clippers. Beginning 2 days later, mice were either treated with 0.2 ml acetone as a control, 3.4 nmol TPA, 2.5 nmol okadaic acid (OA) or 220 nmol chrysarobin (Chry). TPA and OA were applied to the dorsal skin in 0.2 ml acetone twice weekly for 2 weeks, whereas Chry was applied to the dorsal skin in 0.2 ml acetone once weekly for 4 weeks.

Preparation of epidermal protein lysates

Epidermal lysates from age-matched female DBA/2 and C57BL/6 mice were prepared as described previously (30) with minor modifications. Briefly, mice were sacrificed by cervical dislocation at various times after the final acetone or promoting agent treatment. Hair was removed using a depilatory agent and the dorsal skin was excised. The epidermis was scraped into a modified radio-immunoprecipitation assay (RIPA) buffer (50 mM Tris-HCl, pH 7.5, 150 mM NaCl, 1% Triton X-100, 1 mM EDTA, 1 mM PMSF, 0.66 µg/ml aprotinin, 0.5 µg/ml leupeptin, 1 µg/ml pepstatin, 1 mM Na_3VO_4 and 1 mM NaF) under liquid nitrogen and ground to a fine powder using a mortar and pestle. The cell lysates were further homogenized through an 18-gauge needle and then centrifuged at 14000*g* for 15 min at 4°C. Protein concentration of the supernatants was measured using the Bradford assay according to the manufacturer's procedure (Bio-Rad Laboratories, Hercules, CA).

RNA extraction

The RNA extraction protocol was followed as described previously (24) with minor modifications. The epidermis was scraped into RNA later (Qiagen, Valencia, CA) and total RNA from the epidermis of control (acetone-treated) and promoter-treated DBA/2 and C57BL/6 mice was extracted according to the manufacturer's protocol. RNA was quantified by spectrophotometry and sample quality was determined by analysis on a 2100 Bioanalyzer (Agilent Technologies, Santa Clara, CA). RNA was further purified on RNeasy columns (Qiagen) with optional DNase I treatment prior to cDNA synthesis.

Two-dimensional polyacrylamide gel electrophoresis and image analysis

Two-dimensional polyacrylamide gel electrophoresis (2-D PAGE) was performed according to the manufacturer's suggested protocols (Bio-Rad Laboratories) as described previously (31,32) with some minor modifications. Protein extracts (150 µg) were pooled together from six samples per treatment group and precipitated from the RIPA buffer using a Perfect-FOCUS kit (Geno Technology, Inc., St. Louis, MO). For each treatment group, 2-D PAGE was performed on a wide pH range, 3–10, and three narrower pH ranges: 4–7, 5–8 and 7–10. Gel images were captured on a Kodak Image Station 440CF (Eastman Kodak Company, Rochester, NY). Each 2-D gel (per pH range and per treatment group) was repeated using the same samples at least once to ensure technical reproducibility. Quantitative comparisons of integrated signal intensities were performed using Bio-Rad's PDQuest 2-D gel image analysis software program. Differential expression was then confirmed visually by two independent observers. Selected spots were manually excised and subjected to in-gel tryptic digestion based on the procedure described by Rosenfeld *et al*. (33).

Protein identification

The tryptic digests were analyzed on a Voyager-DE PRO matrix-assisted laser desorption/ionization time of flight (MALDI-TOF) mass spectrometer (Applied Biosystems, Foster City, CA) as described previously (31,34). For peptide mass mapping, automated MALDI-TOF spectral acquisition and database searching were performed as described (32,35). When MALDI-TOF was not sensitive enough for certain proteins, LC-MS/MS analysis was used. In this case, digests were resuspended in 20 µl Buffer A (5% acetonitrile, 0.1% formic acid, 0.005% heptafluorobutyric acid [HFBA]) and 3–6 µl loaded onto a 12-cm × 0.075 mm fused silica capillary column packed with 5 µM diameter C-18 beads using a N_2 pressure vessel at 1100 psi. Peptides were eluted by applying a 55 min, 0–80% linear gradient of Buffer B (95% acetonitrile, 0.1% formic acid, 0.005% HFBA) at a flow rate of 130 µl/min with a pre-column flow splitter resulting in a final flow rate of ~200 nl/min directly into the source. An LCQ mass spectrometer (Thermo Finnigan, San Jose, CA) was run in automatic collection mode with an instrument method composed of a single segment and four data-dependent scan events with a full MS scan followed by three MS/MS scans of the highest intensity ions. Normalized collision energy was set at 30, activation Q was 0.250 with a minimum full-scan signal intensity at 5×10^5 and a minimum MS^2 intensity at 1×10^4. Dynamic exclusion was turned on utilizing a three-minute repeat count of 2 with the mass width set at 1.50 Da. Sequence analysis was performed using TurboSEQUEST™ (ThermoFinnigan) or MASCOT (Matrix Sciences, London GB) using an indexed human subset database of the non-redundant protein database from National Center for Biotechnology Information (NCBI) web site (http://www.ncbi.nlm.nih.gov/).

Western blot analysis

For traditional 1-dimentional (1-D) immunoblotting, protein extracts (40 µg) from the epidermis of individual DBA/2 and C57BL/6 mice were electrophoresed through an 8–16% gradient sodium dodecyl sulfate (SDS)-PAGE gel. The 1-D western blot was repeated at least once with the epidermis of a different set of individual DBA/2 and C57BL/6 mice. For 2-D western blotting, protein extracts (150 µg) of pooled DBA/2 and C57BL/6 mice were separated using 2-D PAGE with immobilized pH gradient (IPG) strips of pH 3–10 to cover the maximum pH range, using the running conditions specified above. The separated proteins were then transferred onto polyvinylidene fluoride membranes. Antibodies specific to S100A8 and S100A9 (Santa Cruz Biotechnology, Santa Cruz, CA) were used at a 1:500 dilution. Antibody specific to phospho-NFκB ser536 was from Cell Signaling Technology, Beverly, MA and used at a dilution of 1:1000.

IHC and immunofluorescence analyses

IHC analysis was performed as described previously (36) with some minor modifications. The primary antibodies against S100A8 and S100A9 (Santa Cruz Biotechnology) were both diluted at 1:250. The biotinylated secondary antibody was used at a dilution of 1:250. The expression and localization of phospho-NFκB p65 was determined using immunofluorescence on sections of skin with anti-phospho-NFκb p65 (ser276) antibody (Cell Sigaling Technology, Beverly, MA) as described previously (37). Sections were analyzed using a Leica TCS SP5 X White Light Laser Confocal System.

Real-time quantitative reverse transcriptase PCR (qPCR)

Levels of S100a8, S100a9, Tnf, Nfkb1, Il1b and Il22 mRNA were examined by real-time quantitative reverse transcriptase PCR on an ABI 7900HT Fast Real-Time PCR System (Applied Biosystems) by the TaqMan® primer and probe system. Primers and probe for S100a8 were designed using File Builder 3.1 software to a unique region of the gene and spanned exon–exon junctions. An Assay-on-Demand® was used for the analyses of S100a9 (catalog# Mm00656925_m1), Tnf (Mm00443258_ml), Nfkb1 (Mm00476379_ml), Il1b (Mm01336189_ml) and Il22 (Mm00444241_ml), which were also designed to span exon–exon junctions.

For qPCR analysis transcript levels, 1 µg of epidermal RNA isolated from six mice of each genetic background (DBA/2 and C57BL/6) were reverse transcribed to cDNA by random priming using the Applied Biosystems High-Capacity cDNA Archive Kit (Applied Biosystems) in 50 µl reactions. For qPCR, 2 µl of cDNA were used per assay in a reaction volume of 20 µl and each sample was analyzed in duplicate. Samples were normalized to 18S or β-actin RNA and all qPCR assays were analyzed based on the relative quantification (△△Ct) method. Serial dilutions of RNA from TPA-treated epidermis were used for the construction of relative standard curves for each assay. In all qPCR analyses, control samples processed without reverse transcriptase, as well as no template control samples were included to verify a lack of contaminating genomic DNA in the sample preparations.

Pathways analysis

The 19 proteins identified in the present study were analyzed by IPA (Ingenuity Systems, Mountain View, CA). Briefly, the unique Swiss-Prot accession numbers of the 19 differentially expressed proteins identified were uploaded into IPA, together with their differential expression ratio (DBA/2 over C57BL/6 for both acetone and TPA-treated mice as shown in Table 1). Theoretical protein networks were then constructed, and a score for each possible network (the negative base-10 logarithm of the *P* value) was calculated. Scores of 2 or higher indicated at least a 99% confidence of not being constructed by a random chance.

Statistical analysis

For qPCR, significance of differences in transcript levels was determined using a two-tailed Student's *t* test. For 2-D gel, six biological replicate samples were pooled together as one experimental sample per treatment group. Two technical replicates (experimental repeats) were obtained per pH range and per treatment group. For 2-D gel-based proteomics experiments, because initial 2-D experiments were conducted with pooled samples, statistical analysis was not appropriate. Instead, extensive validation of differential protein expression

Table I. Functional significance and expression trend of the identified proteins

Spot #	Protein ID (Official symbol)	Accession no.	theo MW	Mw (kDa)	theo pI	pI	No. of peptides	% coverage	MOWSE	No. of PSD ions matched	Expression trend DBA/C57BL (ratio)[a]			Comments[b]
											0 h	6 h	24 h	
Calcium-binding proteins														
1	Annexin A1 (Anxa1)	P10107	39	39	6.97	6.23	12/20	42	4.23e5		D>>C	NP	NP	
2	Annexin A1 (Anxa1)	P10107	39	39	6.97	6.48	12/20	41	5.19e5		4.7	9.2	17.6	
3	Annexin A1 (Anxa1)	P10107	39	39	6.97	6.83	4/10	15	506		D<<C	D<<C	D<<C	
4	Parvalbumin α (Pvalb)	P32848	12	13	5.02	4.79	5/20	58	51.7	Mox confirmed, ncbi hro 1-100 kD	1.0	0.6	0.6	W, D
5	Parvalbumin α (Pvalb)	P32848	12	13	5.02	4.66	6	65			1.0	7.9	6.5	W, D
6	S100 calcium-binding protein A8 (S100a8)	P27005	10	10	5.43	5.65	1	24		XCorr: 2.86; deltaCorr: 0.14	NP	3.6	4.6	W, D
7	S100 calcium-binding protein A9 (S100a9)	P31725	13	13	6.65	6.76	2/6	23		MS visual spectral matching, 2Mox confirmed	NP	3.6	3.5	W, D
8	S100 calcium-binding protein A9 (S100a9)	P31725	13	13	6.65	6.70	2/5	23	17.8	MS visual spectral matching, 2Mox confirmed	NP	4.1	6.3	W, D
9	S100 calcium-binding protein A9 (S100a9)	P31725	13	13	6.65	6.44	5/17	38	62.4		NP	24.1	2.4	W, D
10	S100 calcium binding protein A11 (S100a11)	P50543	11	10	5.3	5.32	2/2	27	4.49	8/9	NP	2.0	2.0	D
Microfilament proteins														
11	Profilin 1(Pfn1)	P62962	15	15	8.46	9.15	2/3	16	11.4	14/16	2.4	2.1	1.3	
12	Actin, β and γ(Actb, gamma-actin)	P60711, CAA31455	42	26	5.3	5.46	3/3	10	79.4		1.9	1.0	0.4	
Chaperone proteins														
13	Heat-shock protein beta-1 (Hspb1)	P14602	23	25	6.12	6.18	9/20	37	1.78e5		0.9	0.4	0.5	
14	60 kDa heat-shock protein, Mitochondrial (Hspd1)	P63038	61	60	5.91	5.41	¾	6	41.7	9/11	1.7	1.2	0.5	
15	60 kDa heat-shock protein, Mitochondrial (Hspd1)	P63038	61	60	5.91	5.32	2/2	6	19.3	Same two peptides seen in spot 14	3.6	0.4	0.7	
Proteases and catalytic enzymes														
16	Stefin A3 (Stfa3)	P35175	11	13	5.9	5.62	6/15	68	66		NP	2.2	1.4	
17	Stefin A3 (Stfa3)	P35175	11	13	5.9	5.69	4/15	44	27.3		NP	3.1	1.2	
18	Stefin A3 (Stfa3)	P35175	11	13	5.9	5.88			Visual spectral matching		NP	2.2	2.4	
Fatty-acid- and cholesterol-related proteins														
19	Apolipoprotein A1 (Apoa1)	Q00623	31	22	5.7	5.59	8/15	32	257		D>C	D>>C	D>>C	
20	Apolipoprotein A1 (Apoa1)	Q00623	31	22	5.7	5.24	9/15	31	291		D<C	D<<C	D<<C	
21	Fatty acid–binding protein, epidermal (Fabp5l2)	Q05816	15	15	5.7	6.04	2/3	12%	Visual spectral matching		3.1	1.4	1.3	
22	Fatty-acid-binding protein, adipocyte (Fabp4)	P04117	15	14	5.7	6.18	¾	18%	14.8	15/17	1.4	0.4	1.0	
Signal transduction														
23	14-3-3 σ (Stratifin) (Sfn)	O70456	28	28	4.75	4.57	3/3	12%	Manual analysis		1.4	2.4	1.0	
24	14-3-3 σ (Stratifin) (Sfn)	O70456	28	28	4.75	4.61	3/3	12%	2.99	9/12, 2 Mox confirmed	1.1	NP	NP	
25	14-3-3 σ (Stratifin) (Sfn)	O70456	28	28	4.75	4.65	2/2	8%	Manual analysis	7/11, 2 Mox confirmed	1.4	NP	NP	
Others														
26	α enolase (Eno1)	P17182	47	47	6.37	6.36	7/20	27	3.03e3		0.5	1.7	1.2	
27	α enolase (Eno1)	P17182	47	47	6.37	6.57	6/20	20	177		0.4	1.8	1.5	
28	Major urinary protein 2 precursor (Mup2)	P11589	21	21	5.0	4.62	6/15	40	66		NP	D<<C	NP	
29	Transthyretin (precursor) (Ttr)	P07309	16	15	5.8	6.09	1/1	4	6.7	12/16	NP	0.5	0.4	
30	Lactoyl glutathione lyase (glyoxylase) (Glo1)	Q9CPU0	21	21	5.2	5.10	4/20	14	9.33	14/18	6.1	1.4	2.8	

[a]Ratio of spot intensity between DBA/2 mice versus C57BL/6 mice (D/C), from 2-D gels of pooled samples. The ratios could not be calculated when one or both of the two comparing samples had a zero reading. NP, the spot is not present in both strains of mice. D>>C means that the spot is absent in C57BL/6 mice; and D<<C stands for its absence in DBA/2 mice.

[b]W, differential expression was confirmed by 1-D and/or 2-D western blot analysis and D, discussed in this paper.

was conducted with protein samples from individual mice to compensate for this lack of statistical support.

Results

In the current study, we initially evaluated protein extracts from the epidermis of DBA/2 and C57BL/6 mice treated with TPA using a multiple-treatment regimen. For these analyses, equal amounts of protein extracts from six mice per treatment group were pooled together and separated by 2-D PAGE on a wide pH range of 3–10, and three narrower pH ranges of 4–7, 5–8 and 7–10. Figure 1 shows six selected 2-D gel images of epidermal protein extracts separated on a pH range between 5 and 8. Comparison of 2-D gel images from epidermal protein lysates of TPA- and acetone-treated mice showed that TPA treatment resulted in increased expression of many proteins in both DBA/2 and C57BL/6 mice. Notably, some of these proteins were differentially expressed between the two strains. Among 30 differentially expressed spots representing 19 distinct proteins (Table 1), 10 spots were identified as five distinct calcium-binding proteins (annexin A1, parvalbumin α, S100A8, S100A9 and S100A11). Other represented proteins included two heat-shock proteins (hsp27 and hsp60), a cholesterol transport protein (apolipoprotein A1), two fatty acid binding proteins (epidermal and adipocyte), one cysteine protease inhibitor (stefin 3), and 14-3-3 σ.

The 2-D gel experiments demonstrated that expression of the three S100 calcium-binding proteins S100A8, S100A9 and S100A11 was not detected in the epidermis of acetone-treated DBA/2 or C57BL/6 mice. In contrast, at 6 and 24 h after the last TPA treatment, these three S100 proteins were induced in epidermis of both strains, although to a greater degree in the epidermis of DBA/2 mice than in the C57BL/6 mice (see again Table 1). This was particularly true for S100A8 and S100A9. Supplementary Figure 1A, available at *Carcinogenesis* Online, shows close-ups of the regions of the 2-D gel images in which S100A8 protein (spot #6) was clearly differentially expressed between DBA/2 and C57BL/6 mice at 6 and 24 h post-TPA treatment. Similar results were observed for S100A9 (Supplementary Figure 1B, available at *Carcinogenesis* Online). Interestingly, S100A9 migrated as three spots (spots #7, 8 and 9) with the same molecular weight and slightly different p*I*s. The exact nature of these three spots and the reason(s) for their different p*I*s is not known.

Upregulation and differential expression of S100A8 and S100A9 between DBA/2 and C57BL/6 mice following TPA treatment (as listed in Table 1) was further examined and validated using 1-D and 2-D western blot analyses, IHC analysis and qPCR analysis. Similar to the 2-D gel experiments, 2-D western blot analysis was done using the pooled epidermal protein lysates from DBA/2 and C57BL/6 (six mice per treatment group). For 1-D western blot analysis, epidermal protein lysates from individual DBA/2 and C57BL/6 mouse were used and repeated at least once to ensure experimental reproducibility using the epidermis of a different set of individual DBA/2 and C57BL/6 mice. The results of 2-D (Figure 2A and 2B) and 1-D (Figure 2C and 2D) western blot analyses validated that S100A8 (Figure 2A and 2C) and S100A9 (Figure 2B and 2D) protein could not be detected in the epidermis of acetone-treated DBA/2 and C57BL/6 mice, and that this protein was differentially expressed at 6 and 24 h post-TPA treatment. Analysis by 2-D western blot also demonstrated that S100A8 existed as a single spot, whereas S100A9 existed as three spots.

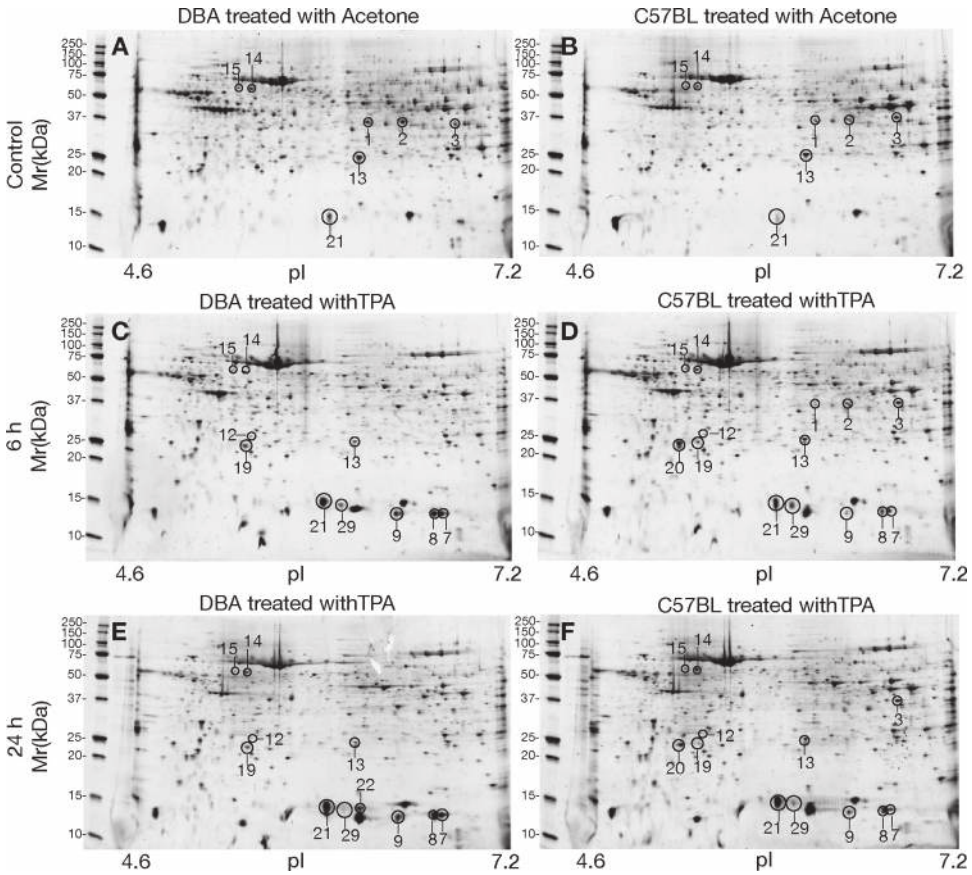

Fig. 1. Selected 2-D gel images of epidermal proteins of DBA/2 and C57BL/6 mice run on IPG (immobilized pH gradient) strips of pH 5–8. The backs of DBA/2 (A, C, E) and C57BL/6 (B, D, F) mice were treated with 3.4 nmol TPA twice weekly for 2 weeks and sacrificed 6 h (C, D) or 24 h (E, F) later. Control mice were treated with acetone (0.2 ml) twice weekly for 2 weeks and sacrificed 6 h later (A, B). Protein extracts (150 µg) were pooled together in equal amounts from six samples of individual mice per treatment group. Two technical replicates from the same samples (technical repeats) were obtained per pH range and per treatment group to ensure experimental reproducibility.

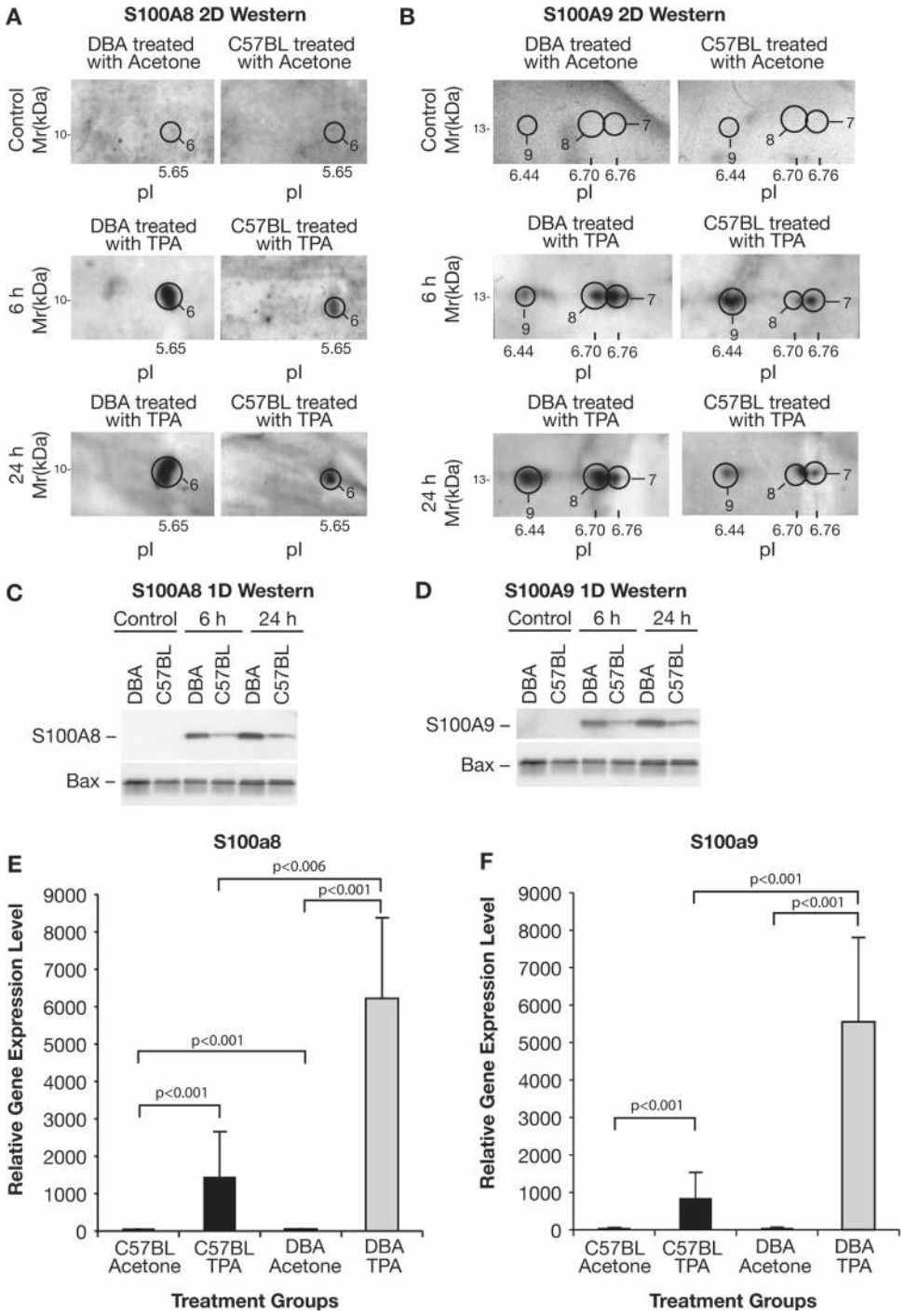

Fig. 2. Validation of epidermal S100A8 and S100A9 levels after twice weekly treatments for 2 weeks with 3.4 nmol TPA. Two-dimensional western blot analysis of (**A**) S100A8 and (**B**) S100A9 in the pooled epidermis of DBA/2 and C57BL/6 mice with acetone, and 6 or 24 h post TPA treatment, as indicated. One-dimensional western blot analysis of (**C**) S100A8 and (**D**) S100A9 in the epidermal lysates of individual DBA/2 and C57BL/6 mice, with acetone treatment as controls, and 6 or 24 h post TPA treatment, as indicated. One-dimensional western blot analysis was repeated at least once to ensure experimental reproducibility with lysates from the epidermis of a different set of individual DBA/2 and C57BL/6 mice. Sample types and treatments are as labeled. Protein spot number indicated is the same as that in Table 1. The protein level of Bax was used as a loading control as indicated. Real-time qPCR analysis of S100a8 (**E**) and S100a9 (**F**) mRNA levels in the epidermis from mice sacrificed 24 h after the last of four TPA treatments. Bars represent the relative mRNA levels of S100a8 and S100a9 normalized to 18S RNA from either TPA- or acetone-treated epidermis of DBA/2 and C57BL/6 mice as indicated. Each bar represents an average of six individual mice of each genetic background analyzed in duplicate in separate experiments. Data is shown as the ratios of fold differences in mRNA levels, relative to the acetone-treated C57BL/6 samples.

As shown in Figure 2E, qPCR analysis of individual epidermal RNA samples from the 24-h time point indicated that S100a8 mRNA levels were very low in the epidermis of acetone-treated DBA/2 and C57BL/6 mice. However, S100a8 mRNA was detected in the epidermis of both C57BL/6 and DBA/2 mice 24 h after the final TPA treatment. Furthermore, S100a8 mRNA levels were significantly higher

(~4-fold) in epidermis of DBA/2 mice compared with C57BL/6 mice ($P < 0.001$). S100a9 mRNA levels before and after TPA treatment exhibited a similar pattern as shown in Figure 2F with mRNA levels approximately 5-fold higher ($P < 0.001$) in the epidermis of TPA-treated DBA/2 mice compared with C57BL/6 mice.

In the next series of experiments, a longer time course was conducted to further study the protein expression of S100A8 and S100A9 using both 1-D western blot analysis and IHC analysis. For western blot analysis, the epidermal protein lysates from acetone or TPA-treated DBA/2 and C57BL/6 mice were pooled in equal amounts from four mice per group. As shown in Figure 3A, TPA treatment induced the expression of these proteins in both strains of mice, reaching the maximum protein level between the 24-h and 72-h time points. Again, higher protein levels for both proteins were observed in the epidermis of TPA-treated DBA/2 mice compared with C57BL/6 mice. Although S100A9 protein was still detectable 96 h after TPA treatment in the epidermis of both C57BL/6 and DBA/2 mice, S100A8 protein could not be detected at this time point. In contrast, S100A10 protein was

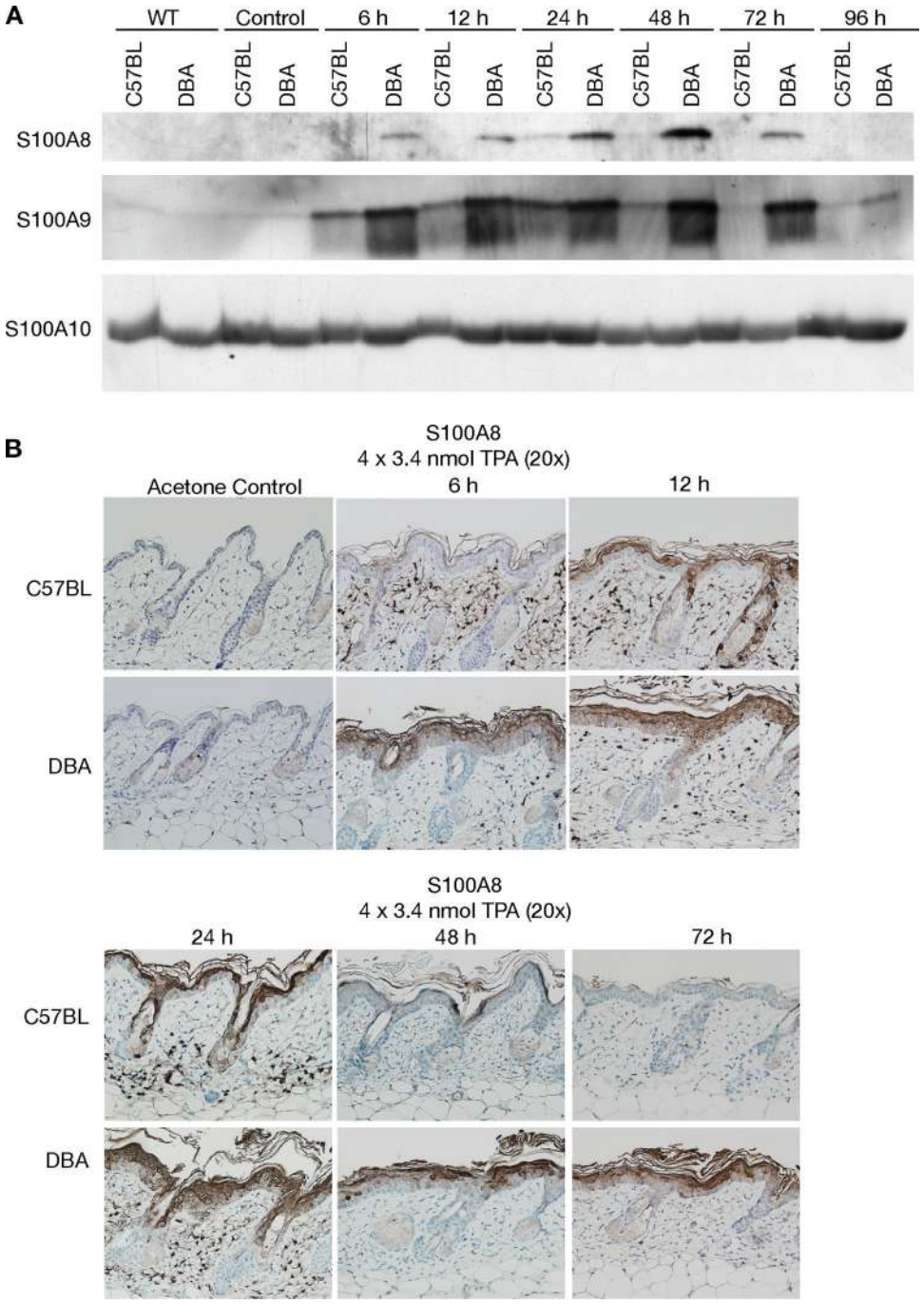

Fig. 3. Time course of S100A8 and S100A9 protein level changes following TPA treatment. (**A**) one-dimensional western blot analysis of S100A8 and S100A9. Pooled epidermal protein samples of DBA/2 and C57BL/6 (four mice per group) were loaded in equal amounts in each lane as indicated. The time points following the last TPA treatment are as indicated. WT and control represent no treatment and acetone treatment, respectively. S100A10 was also analyzed and used here as a loading control. (**B**) IHC analysis of S100A8 as described in 'Materials and methods' section. The time points following the last TPA treatment are as indicated. All IHC images were photographed at a magnification of ×20.

expressed at about the same level in all samples and was used as a sample loading control. As shown in Figure 3B, IHC analysis further confirmed that S100A8 protein was not detectable in the epidermis of acetone-treated DBA/2 and C57BL/6 mice but was induced by TPA treatment to a much greater degree in epidermis of TPA-treated DBA/2 mice compared with C57BL/6 mice. Figure 3B further demonstrates that S100A8 protein expression reached the maximum level between the 24-h and 72-h time points, which is consistent with the results of 1-D western blot analysis. It can also be seen from the IHC data shown in Figure 3B that S100A8 staining was observed primarily in the suprabasal layer of the epidermis; similar results were observed for S100A9 staining (data not shown).

One-dimensional western blot analysis was also used to determine S100A8 and S100A9 protein levels in the epidermis of C57BL/6 and DBA/2 mice treated with OA and Chry, two other skin tumor promoting agents whose initial biochemical mechanism of action is different from that of the phorbol ester TPA [reviewed in ref. 2]. For these experiments, equal amounts of epidermal protein samples were pooled from three mice per group and then loaded onto gels. As shown in Supplementary Figure 2A, available at *Carcinogenesis* Online, S100A8 and S100A9 protein levels were higher in the epidermis of DBA/2 than C57BL/6 mice treated with OA at all time points examined. Similar results were observed for S100A8 protein expression in mice treated with Chry (Supplementary Figure 2B, available at *Carcinogenesis* Online). Following treatment with Chry, S100A9 protein levels were similar in the epidermis of DBA/2 and C57BL/6 mice (Supplementary Figure 2B, available at *Carcinogenesis* Online) at 6 and 18 h after the last treatment, whereas at later time points (24 and 48 h), S100A9 protein levels were again higher in the epidermis of DBA/2 compared with C57BL/6 mice.

To further explore the observed differences in protein levels between DBA/2 and C57BL/6 mice, IPA software was used to map the differentially expressed proteins into two biological networks for each treatment group (acetone control and 6 or 24 h after the last TPA treatment). Supplementary Table 1, available at *Carcinogenesis* Online lists these six biological networks (Networks 1–6) with highly significant scores of 27, 4, 32, 16, 32 and 13, respectively. Mapped within these six networks were 10, 2, 12, 7, 12 and 6 focus proteins, respectively, from the differentially expressed proteins identified in the present study. The most significant networks identified by IPA incorporated 12 focus proteins (out of the total 19 differentially expressed proteins identified) with the score of 32 at both 6 and 24 h after the last TPA treatment (Networks 3 and 5, Figures 4A and 4B, respectively). The top functions for the most significant network at the 6-h time point (Network ID 3 in Supplementary Table 1, available at *Carcinogenesis* Online and Figure 4A) were cellular movement, antigen presentation and cell-mediated immune response. The most significant functions of the highest score network at the 24-h time point (Network ID 5 in Supplementary Table 1, available at *Carcinogenesis* Online, and Figure 4B) were lipid metabolism, molecular transport and small-molecule biochemistry. It is interesting to note that both Networks 3 and 5 contain a number of inflammation-associated proteins including NFκB, IL-22 and p38 MAPK.

Supplementary Figure 3, available at *Carcinogenesis* Online, displays the other IPA Networks listed in Supplementary Table 1, available at *Carcinogenesis* Online. Notably, the next most significant networks obtained at 6 and 24 h following TPA treatment again contained inflammation-associated proteins, including TNF-α (Networks 4 and 6, Supplementary Figure 3A and B, available at *Carcinogenesis* Online, respectively). The most significant network observed in acetone-treated mice is shown in Supplementary Figure 3C, available at *Carcinogenesis* Online, and again contained a number of inflammation-associated genes. When only the five differentially expressed calcium-binding proteins identified from the present study (ANXA1, PVALB, S100A8, S100A9 and S100A11) were uploaded into IPA software, they were mapped to a biological network of cancer or cell-to-cell signaling and interaction (Network ID 7 in Supplementary Table 1 and Supplementary Figure 3E, available at *Carcinogenesis* Online). Within this network, an additional 19 proteins and/or molecules were identified, including two other calcium-binding proteins, ANXA2 and ANXA5, as well as Pkc(s) and FActin, which are connected with the five differentially expressed calcium-binding proteins.

The presence of several inflammation-associated proteins (including NFκB, TNF-α, p38 MAPK and IL-22) in the interaction networks identified led to follow-up studies. For these studies, qPCR was used to examine mRNA expression levels of two of the above inflammation-associated genes (*Tnf* and *Il22*) in epidermal RNA samples from DBA/2 and C57BL/6 mice at both 6 and 24 h after the last of four TPA treatments. Two other NFκB-regulated genes, *Il1b* and *Nfkb1*, were also included in these initial analyses (38). As shown in Figure 5A, Il22 mRNA (found in Network IDs 3 and 7, Supplementary Table 1, available at *Carcinogenesis* Online, Figure 4A, and Supplementary Figure 3E, available at *Carcinogenesis* Online) was approximately 100-fold higher in the epidermis of TPA-treated DBA/2 mice compared with the mRNA levels in TPA-treated C57BL/6 epidermis (24-h time point; Figure 5A). Il22 mRNA was also differentially expressed significantly at the 6-h time point (DBA/2>>C57BL/6 with $P < 0.001$; data not shown). In contrast, Nfkb1 (Networks 3 and 5, Supplementary Table 1, available at *Carcinogenesis* Online) mRNA levels were induced in epidermis of both TPA-treated DBA/2 and C57BL/6 mice to approximately similar levels at the 6-h time point (data not shown). However, at the 24-h time point, Nfkb1 mRNA level remained elevated in epidermis of TPA-treated DBA/2 mice but returned to near control levels in epidermis of C57BL/6 mice, resulting in ~2.5-fold higher level in epidermis of TPA-treated DBA/2 mice at this time point (Figure 5B). A similar pattern was observed for Tnf mRNA (Network 4, Supplementary Table 1 and Supplementary Figure 3A, available at *Carcinogenesis* Online). In this regard, Tnf mRNA was induced to a similar extent in epidermis of both DBA/2 and C57BL/6 mice at the 6-h time point (again data not shown). At 24 h after the last TPA treatment, Tnf mRNA remained elevated in the epidermis of DBA/2 mice but returned to below control levels in epidermis of C57BL/6 mice leading to an approximately 7-fold higher level in the epidermis of TPA-treated DBA/2 mice at this time point (Figure 5C). Finally, Il1b transcript levels were induced by TPA to a similar level at 6 h in epidermis of both strains (data not shown). Again as with Nfkb1 and Tnf, Il1b mRNA levels decreased in epidermis of C57BL/6 mice at the 24-h time point (although still significantly above the C57BL/6 acetone control) (Figure 5D) but remained elevated in the epidermis of TPA-treated DBA/2 mice resulting in an 8-fold higher level at this time point. The differences in levels of mRNAs for Il22, Nfkb1, Tnf and Il1b observed between epidermis of TPA-treated DBA/2 and C57BL/6 mice at the 24-h time point were statistically significant ($P < 0.001$) in all cases.

In light of the differences noted above (and shown in Figure 5 panels A–D), we analyzed several other NFκB-regulated genes (*Cxcl1*, *Cxcl2* and *Cxcl5*) (39,40) for their mRNA levels in epidermis of DBA/2 and C57BL/6 mice after treatment with TPA. As shown in Figure 5E, Cxcl1 mRNA levels increased to approximately the same extent in epidermis of both strains of TPA-treated mice at the 6-h time point (differences not statistically significant, $P > 0.05$). However, at the 24-h time point, Cxcl1 mRNA levels decreased to near control levels in epidermis of C57BL/6 mice while remaining at a high level in epidermis of DBA/2 mice. Thus, at the 24-h time point, there was an ~16.6-fold higher level of Cxcl1 mRNA in the epidermis of TPA-treated DBA/2 mice compared with TPA-treated C57BL/6 mice. This pattern of mRNA expression was surprisingly similar to that observed for Il22, Nfkb1, Tnf and Il1b, where the greatest differences in mRNA levels were observed at the 24-h time point. Similarly, at the 6-h time point following the last of four TPA treatments, both Cxcl2 and Cxcl5 mRNA levels increased to the same extent in epidermis of both strains of mice (Figure 5F and 5G, respectively). Again, Cxcl2 and Cxcl5 mRNA levels returned to near control levels in epidermis of TPA-treated C57BL/6 at the 24-h time point while mRNA levels for both of these genes remained elevated in epidermis of DBA/2 mice. Thus, at the 24-h time point, there was an ~ 97-fold higher Cxcl2 mRNA level in epidermis of TPA-treated DBA/2 mice compared with C57BL/6 mice (Figure 5F) and for Cxcl5 an ~ 19-fold higher

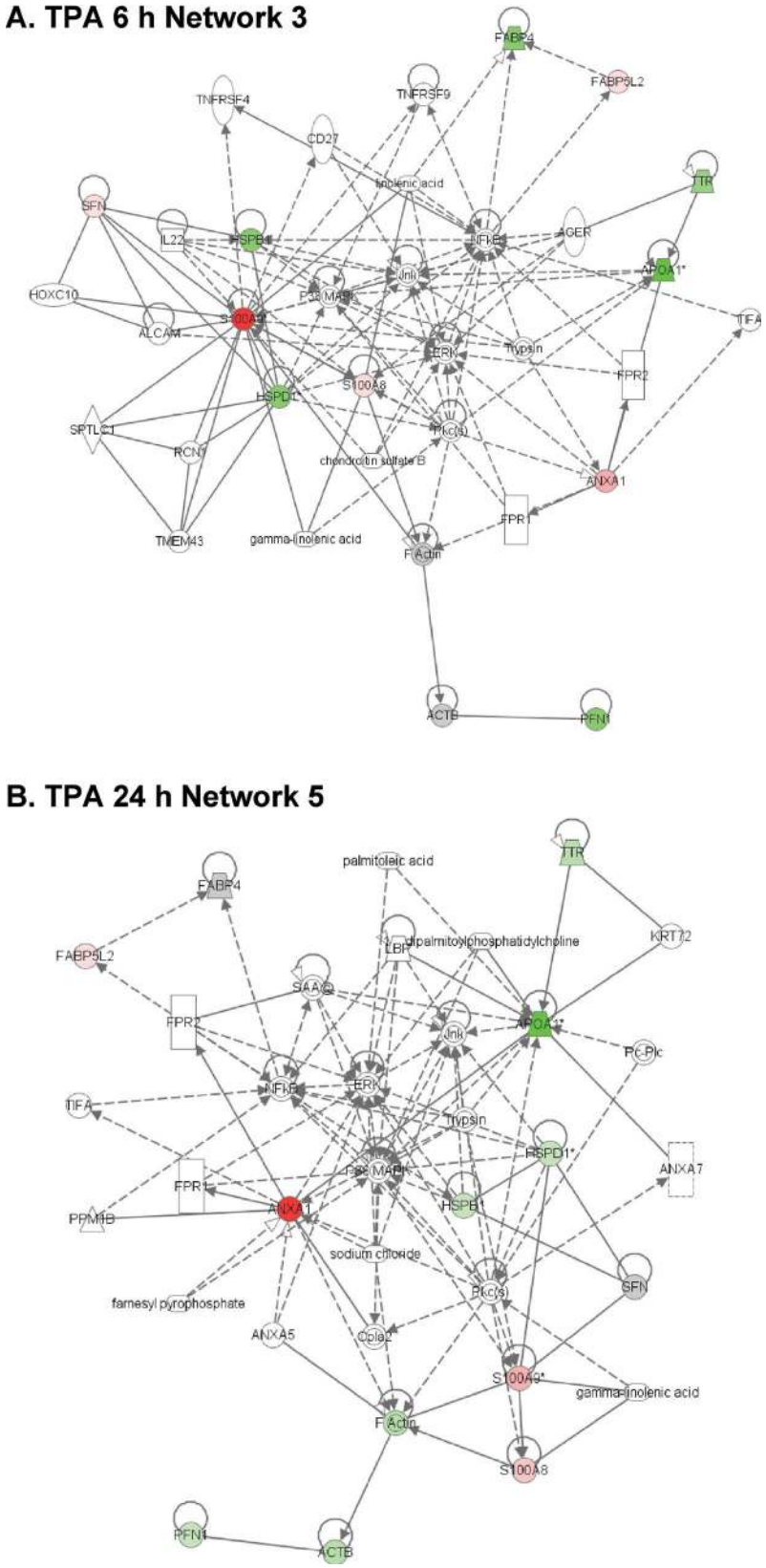

Fig. 4. IPA pathway analysis of the differentially expressed proteins identified from 2-D gel-based proteomics experiments. (**A**) Network 3 (Supplementary Table 1, available at *Carcinogenesis* Online) is the most significant network identified for the 6-h time point after the last TPA treatment. Several inflammatory proteins, including NFκB, p38 MAPK and IL-22, are implicated in this network. (**B**) Network 5 (Supplementary Table 1, available at *Carcinogenesis* Online) is identified as the most significant network 24 h after the last TPA treatment. In this network, inflammatory proteins including NFκB and p38 MAPK are again suggested to be involved. Molecules identified as differentially expressed from 2-D gel-based proteomics experiments (as shown in Table 1) are colored.

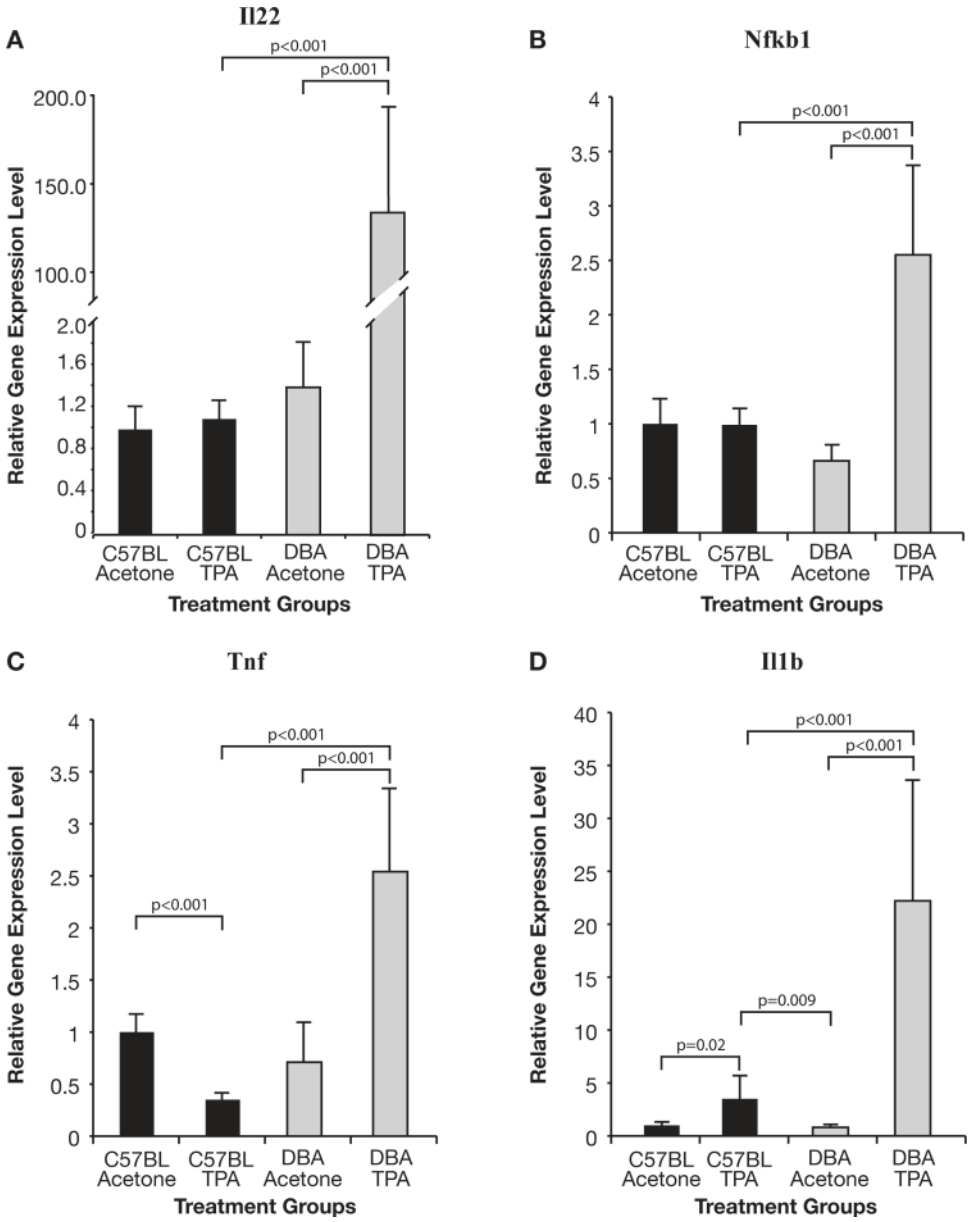

Fig. 5. qPCR analyses of epidermal mRNA levels NFκB (p65) and induction of NFκB-regulated cytokines and chemokines. Bars represent relative mRNA levels of Il22 (**A**), Nfkb1 (**B**), Tnf (**C**) and Il1b (**D**) normalized to 18S RNA, and Cxcl1 (**E**), Cxcl2 (**F**) and Cxcl5 (**G**) normalized to β-actin mRNA in either TPA- or acetone-treated epidermis of DBA/2 and C57BL/6 mice as indicated. All mice were sacrificed 24 h post acetone or TPA treatment. Each bar represents an average of six individual mice of each genetic background analyzed (in duplicate in separate experiments). Data are shown as fold differences in mRNA levels relative to the acetone-treated C57BL/6 samples. Panel H shows immunofluorescence staining of skin sections for phospho-p65 (ser276) from mice sacrificed 24 h after the last of four treatments with TPA.

mRNA level in TPA-treated DBA/2 mice compared with TPA-treated C57BL/6 mice (Figure 5G). All differences at the 24-h time point were highly significant ($P < 0.001$ for Cxcl1; $P < 0.001$ for Cxcl2; and $P = 0.006$ for Cxcl5).

Previous studies have shown that TPA induces activation (i.e. phosphorylation) of NFκb (p65) in mouse epidermis within 1 h after topical treatment (41–44). Consistent with the more prolonged induction of Il22, Nfkb1, Tnf, Il1b, Cxcl1, Cxcl2 and Cxcl5 mRNAs in epidermis of DBA/2 mice, we found a sustained activation of NFκB (phospho-p65) in epidermis of DBA/2 mice compared with C57BL/6 mice. This was shown by western blotting (phospho-p65 ser536; Supplementary Figure 4, available at *Carcinogenesis* Online) and by immunofluorescence staining of skin sections for phospho-p65 (ser276) as shown in Figure 5H. Twenty-four hours after TPA treatment, few epidermal keratinocytes with nuclear staining for phospho-p65 could be seen in skin sections from C57BL/6 mice. In contrast, approximately 30–40% of the cells in the epidermis of DBA/2 mice had nuclei that stained positive for phospho-p65 (again see Figure 5H). Thus, the activation of NFκB paralleled the changes in mRNA levels observed for genes regulated by this transcription factor.

Discussion

The present study utilized protein expression profiling to further identify differentially expressed proteins in the epidermis of tumor promotion-sensitive DBA/2 and resistant C57BL/6 mice following multiple treatments with the phorbol ester tumor promoter, TPA. A total of 19 different proteins were found to be differentially expressed

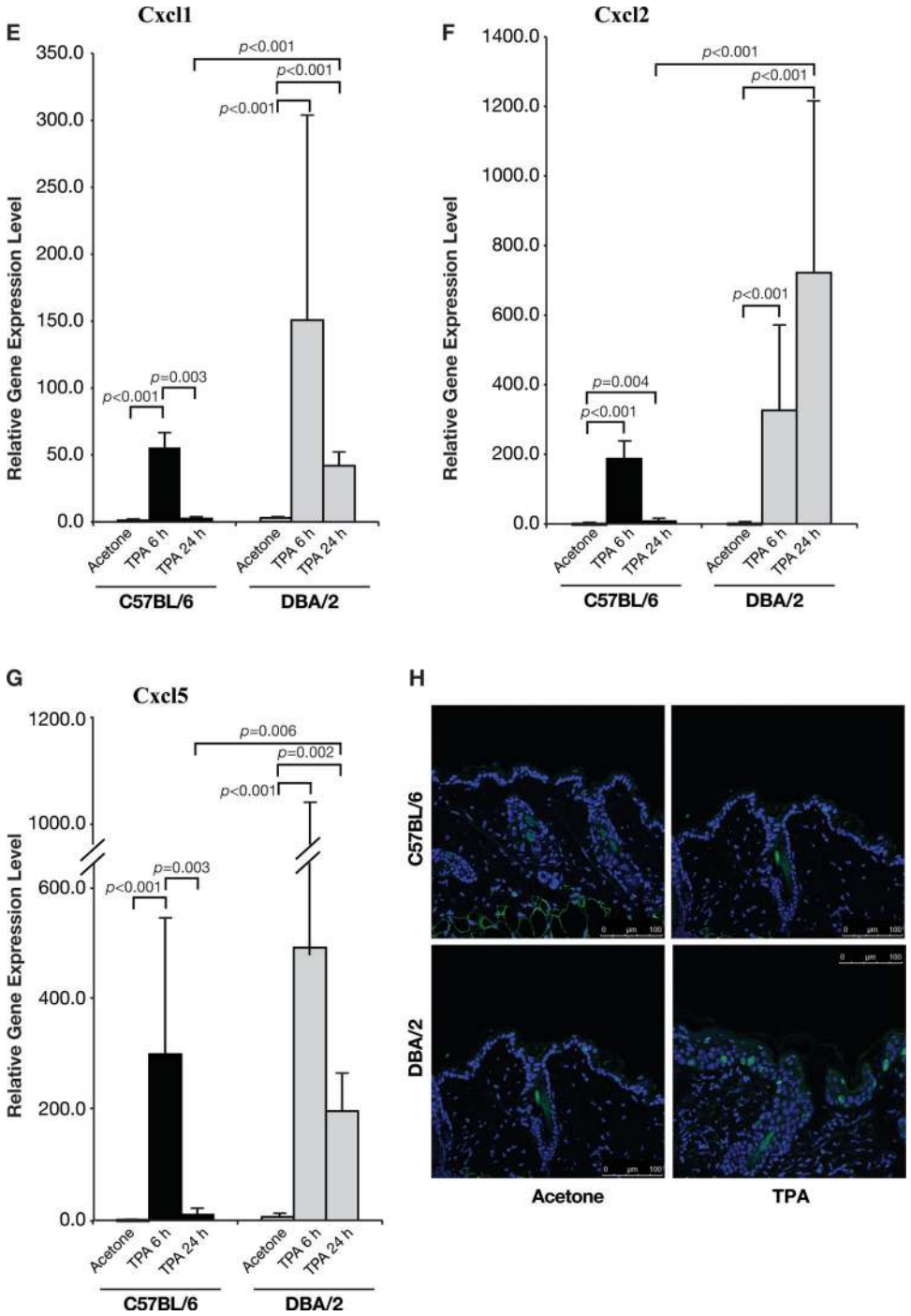

Fig. 5. *Continued*

following TPA treatment. Of these 19 proteins, five calcium-binding proteins including S100A8 and S100A9 were found to be differentially expressed between the epidermis of DBA/2 and C57BL/6 mice 6 and 24 h after the last TPA treatment. Further analyses revealed that S100A8 and S100A9 protein levels were also differentially upregulated in epidermis of DBA/2 versus C57BL/6 mice following topical treatment with two other tumor promoters, OA and Chry. Pathway analysis of all 19 proteins identified in the present study suggested that altered expression of several additional inflammation-related proteins (including TNF-α, NFκB and IL-22) in epidermis following TPA treatment might contribute to skin tumor promotion susceptibility in DBA/2 mice. Follow-up studies revealed that Tnf, Nfkb1, Il22, Il1b, Cxcl1, Cxcl2 and Cxc15 mRNAs were present at significantly higher levels in epidermis of DBA/2 compared with C57BL/6 mice at 24 h following treatment with TPA. Further analyses revealed that NFκB was highly activated in epidermal keratinocytes of DBA/2 but not C57BL/6 mice at the 24 h after TPA treatment. Collectively, the present data suggest that differential expression of inflammation-related genes in the epidermis may play a role in the differential susceptibility of DBA/2 and C57BL/6 mice to skin tumor promotion by TPA and possibly other skin tumor promoters.

The S100A8 and S100A9 proteins belong to the S100 calcium-binding protein family, which has more than 20 members that are involved in regulating differentiation, transcription, cell cycle, cell

growth and motility (45). In the current study, S100A8 and S100A9 were not detected in the epidermis of acetone-treated controls, consistent with a previous finding of their minimal mRNA expression in normal epidermis (46). Both proteins were induced in the epidermis of DBA/2 and C57BL/6 mice within 6 h after the last of four treatments with TPA, with higher protein expression seen in epidermis of DBA/2 mice as noted above. Differential transcript and protein levels between DBA/2 and C57BL/6 mice were further examined and confirmed by qPCR, 1-D and 2-D western blot analyses, and IHC analysis (see Figures 2 and 3 and Supplementary Figure 2, available at *Carcinogenesis* Online). TPA treatment was shown previously to induce S100a8 and S100a9 mRNAs in murine epithelial cells and epidermis (22). We also reported the upregulation of S100a8 and S100a9 mRNAs in the epidermis of DBA/2 and C57BL/6 mice treated with TPA; however, differential mRNA expression of either gene between these two strains of mice was not observed in this earlier microarray study (6-h time point) (24). The current results indicate that both *S100a8* and *S100a9* are differentially expressed in the epidermis at both the mRNA and protein levels at 24 h after the last TPA treatment in a concordant manner. A role for S100 proteins, particularly S100A8 and S100A9 in inflammation and cancer, including the mouse skin carcinogenesis model, has been suggested by a number of observations (29,47–49).

Differences in the epidermal hyperplasia response and the dermal inflammatory response following topical treatment with TPA to various mouse strains have been known for many years (reviewed in refs. 3,25). Sisskin *et al*. (50) first reported that, after multiple TPA treatments, DBA/2 mice displayed a potentiated epidermal hyperplasia, whereas C57BL/6 mice showed only moderate epidermal hyperplasia. Lewis and Adams (51) reported that TPA treatment of C57BL/6 mice induced dermal infiltration of only a very small number of polymorphonuclear leukocytes compared with SENCAR mice. Further work from our laboratory confirmed differences between DBA/2 and C57BL/6 mice in terms of both epidermal hyperplasia and cell proliferation, as well as dermal inflammation as assessed by inflammatory infiltrate, using a regimen of multiple TPA treatments (52,53). In those studies, the correlation between the degree of sustained epidermal hyperplasia and proliferation, as well as skin inflammation and inherited susceptibility to tumor promotion was established (50,53). An interesting observation in the current study was the identification of several networks of differentially expressed proteins containing several inflammation-associated proteins. These proteins included NFκB (p65), TNF-α, p38 MAPK and IL-22. Follow-up studies revealed that the mRNA levels for genes encoding two of these proteins, as well as *Il1b* and Nfkb1, were significantly elevated in epidermis of TPA-treated DBA/2 mice compared with C57BL/6 mice at 24 h after the last TPA treatment (Figure 5). Previous studies have demonstrated an important role for *Tnf* in skin tumor promotion. In this regard, *Tnf* knockout (KO) mice are resistant to skin tumor promotion by TPA (54,55). NFκB is known to regulate a number of pro-inflammatory cytokines including TNF-α, IL-1, IL-22 and others (38). As shown in Figure 5, *Nfkb1* (which encodes p100/p50) was significantly upregulated in epidermis of DBA/2 mice compared with C57BL/6 mice following TPA treatment. Furthermore, mRNA levels of the CXCR2 ligands, Cxcl1, Cxcl2, and Cxcl5 were also significantly upregulated in epidermis of DBA/2 mice compared with C57BL/6 mice at 24 h following the last TPA treatment. These CXCR2 ligands are also known to be regulated by NFκB signaling (56,57). NFκB is known to be activated in mouse epidermis early (within 1 h) following topical treatment with TPA (41–44). Our current results demonstrate that there is a more sustained activation of NFκB in the epidermis of DBA/2 mice compared with C57BL/6 mice. Taken together, the current data suggest that differential expression of multiple pro-inflammatory genes in the epidermis may underlie, at least in part, the basis for susceptibility to skin tumor promotion in DBA/2 and C57BL/6 mice. These differences in gene and protein expression in the epidermis may help to drive differences seen in the dermal inflammatory response characteristic of these two strains during the process of tumor promotion.

In summary, using the 2-D gel electrophoresis and MS-based proteomics approach, we identified 19 distinct proteins differentially expressed between mice sensitive (DBA/2) and resistant (C57BL/6) to skin tumor promotion by TPA. This included five distinct calcium-binding proteins. Increased levels of S100a8 and S100a9 transcript and protein, especially in TPA-treated epidermis of DBA/2 mice, was further characterized and correlated with susceptibility to skin tumor promotion with TPA and two other distinct classes of tumor promoters. IPA analyses of the differentially expressed proteins revealed networks that included other inflammation-associated proteins known to be involved in skin tumor promotion. Further analyses demonstrated differential expression of Nfkb1, Tnf, Il22, Il1b, Cxcl1, Cxcl2 and Cxcl5 mRNAs with higher expression in the epidermis of sensitive DBA/2 mice at 24 h after TPA treatment compared with resistant C57BL/6 mice. This prolonged induction of inflammatory cytokines and chemokines was associated with prolonged and elevated epidermal NFκB activity (nuclear phospho-p65). Thus, differences in NFκB signaling may be responsible, at least in part, for the differences seen in inflammatory gene expression. Recently, Quigley *et al*. (58) have identified a locus on chr15 that influences expression of inflammation-associated genes (including genes encoding IL-1R ligands) and susceptibility to skin tumor (papilloma) formation. Our current data indicate that the genetic differences in susceptibility to skin tumor promotion between DBA/2 and C57BL/6 mice may include a much broader network of pro-inflammatory genes, including those known to be directly involved in the process of skin tumor promotion. Further ongoing studies are exploring the role of such pro-inflammatory genes in genetic susceptibility to skin tumor promotion.

Supplementary material

Supplementary Table 1 and Figures 1–4 can be found at http://carcin.oxfordjournals.org/

Funding

National Institutes of Health (R01 ES015718 to J.D., U01 CA098028 to O.J.S.), UTMDACC Core (CA016672) and National Institute of Environmental Health Sciences (ES007784).

Acknowledgments

We thank Kevin Lin for statistical analysis, Vanessa Floyd and Lauren Pascale for preparation of the manuscript and Joi Holcomb for help with the illustrations.

Conflict of Interest Statement: None declared.

References

1. Boutwell,R.K. (1964) Some biological aspects of skin carcinogenisis. *Prog. Exp. Tumor Res.*, **19**, 207–250.
2. DiGiovanni,J. (1992) Multistage carcinogenesis in mouse skin. *Pharmacol. Ther.*, **54**, 63–128.
3. Naito,M. *et al.* (1989) Genetic background and development of skin tumors. *Carcinog. Compr. Surv.*, **11**, 187–212.
4. Bangrazi,C. *et al.* (1990) Genetics of chemical carcinogenesis. 1. Bidirectional selective breeding of susceptible and resistant lines of mice to two-stage skin carcinogenesis. *Carcinogenesis*, **11**, 1711–1719.
5. Saran,A. *et al.* (2000) Genetics of chemical carcinogenesis: analysis of bidirectional selective breeding inducing maximal resistance or maximal susceptibility to 2-stage skin tumorigenesis in the mouse. *Int. J. Cancer.*, **88**, 424–431.
6. Ashman,L.K. *et al.* (1982) Two-stage skin carcinogenesis in sensitive and resistant mouse strains. *Carcinogenesis*, **3**, 99–102.
7. DiGiovanni,J. *et al.* (1984) DBA/2 mice are as sensitive as SENCAR mice to skin tumor promotion by 12-O-tetradecanoylphorbol-13-acetate. *Carcinogenesis*, **5**, 1493–1498.

8. DiGiovanni,J. *et al.* (1980) Comparison of the tumor-initiating activity of 7,12-dimethylbenz[a]anthracene and benzo[a]pyrene in female SENCAR and CS-1 mice. *Carcinogenesis*, **1**, 381–389.
9. Angel,J.M. *et al.* (1997) Association of a murine chromosome 9 locus (Psl1) with susceptibility to mouse skin tumor promotion by 12-O-tetradecanoylphorbol-13-acetate. *Mol. Carcinogen.*, **20**, 162–167.
10. Angel,J.M. *et al.* (2001) Confirmation of the mapping of a 12-O-tetradecanoylphorbol-13-acetate promotion susceptibility locus, Psl1, to distal mouse chromosome 9. *Mol. Carcinogen.*, **32**, 169–175.
11. Angel,J.M. *et al.* (2003) Identification of novel genetic loci contributing to 12-O-tetradecanoylphorbol-13-acetate skin tumor promotion susceptibility in DBA/2 and C57BL/6 mice. *Cancer. Res.*, **63**, 2747–2751.
12. Ewart-Toland,A. *et al.* (2003) Identification of Stk6/STK15 as a candidate low-penetrance tumor-susceptibility gene in mouse and human. *Nat. Genet.*, **34**, 403–412.
13. Ewart-Toland,A. *et al.* (2005) Aurora-A/STK15 T+91A is a general low penetrance cancer susceptibility gene: a meta-analysis of multiple cancer types. *Carcinogenesis*, **26**, 1368–1373.
14. Mao,J.H. *et al.* (2006) Genetic variants of Tgfb1 act as context-dependent modifiers of mouse skin tumor susceptibility. *Proc. Natl. Acad. Sci. USA.*, **103**, 8125–8130.
15. Nagase,H. *et al.* (1995) Distinct genetic loci control development of benign and malignant skin tumours in mice. *Nat. Genet.*, **10**, 424–429.
16. Nagase,H. *et al.* (1999) A subset of skin tumor modifier loci determines survival time of tumor-bearing mice. *Proc. Natl. Acad. Sci. USA.*, **96**, 15032–15037.
17. Saran,A. *et al.* (2004) Loss of tyrosinase activity confers increased skin tumor susceptibility in mice. *Oncogene*, **23**, 4130–4135.
18. Manenti,G. *et al.* (2000) A cancer modifier role for parathyroid hormone-related protein. *Oncogene*, **19**, 5324–5328.
19. Mock,B.A. *et al.* (1998) Multigenic control of skin tumor susceptibility in SENCARA/Pt mice. *Carcinogenesis*, **19**, 1109–1115.
20. Fujiwara,K. *et al.* (2007) New chemically induced skin tumour susceptibility loci identified in a mouse backcross between FVB and dominant resistant PWK. *BMC Genet.*, **8**, 39.
21. Stern,M.C. *et al.* (2002) Genetic analyses of mouse skin tumor progression susceptibility using SENCAR inbred derived strains. *Mol. Carcinogen.*, **35**, 13–20.
22. Schlingemann,J. *et al.* (2003) Profile of gene expression induced by the tumour promotor TPA in murine epithelial cells. *Int. J. Cancer*, **104**, 699–708.
23. Wei,S.J. *et al.* (2003) Identification of Dss1 as a 12-O-tetradecanoylphorbol-13-acetate-responsive gene expressed in keratinocyte progenitor cells, with possible involvement in early skin tumorigenesis. *J. Biol. Chem.*, **278**, 1758–1768.
24. Riggs,P.K., *et al.* (2005) Differential gene expression in epidermis of mice sensitive and resistant to phorbol ester skin tumor promotion. *Mol. Carcinog.*, **44**, 122–136.
25. Angel,J.M. *et al.* (1999) Genetics of skin tumor promotion. *Prog. Exp. Tumor Res.*, **35**, 143–157.
26. Abel,E.L. *et al.* (2010) Evidence that Gsta4 modifies susceptibility to skin tumor development in mice and humans. *J Natl Cancer Inst*, **102**, 1663–1675.
27. Shen,J. *et al.* (2007) Protein expression profiles in the epidermis of cyclooxygenase-2 transgenic mice by 2-dimensional gel electrophoresis and mass spectrometry. *J. Proteome. Res.*, **6**, 273–286.
28. Shen,J. *et al.* (2007) Differential expression of multiple anti-apoptotic proteins in epidermis of IGF-1 transgenic mice as revealed by 2-dimensional gel electrophoresis/mass spectrometry analysis. *Mol. Carcinogen.*, **46**, 331–340.
29. Gebhardt,C. *et al.* (2006) S100A8 and S100A9 in inflammation and cancer. *Biochem. Pharmacol.*, **72**, 1622–1631.
30. DiGiovanni,J. *et al.* (2000) Constitutive expression of insulin-like growth factor-1 in epidermal basal cells of transgenic mice leads to spontaneous tumor promotion. *Cancer Res.*, **60**, 1561–1570.
31. Liu,J.W. *et al.* (2003) Annexin II expression is reduced or lost in prostate cancer cells and its re-expression inhibits prostate cancer cell migration. *Oncogene*, **22**, 1475–1485.
32. Shen,J. *et al.* (2004) Protein expression profiles in pancreatic adenocarcinoma compared with normal pancreatic tissue and tissue affected by pancreatitis as detected by two-dimensional gel electrophoresis and mass spectrometry. *Cancer Res.*, **64**, 9018–9026.
33. Rosenfeld,J. *et al.* (1992) In-gel digestion of proteins for internal sequence analysis after one- or two-dimensional gel electrophoresis. *Anal. Biochem.*, **203**, 173–179.
34. Person,M.D. *et al.* (2003) Comparative identification of prostanoid inducible proteins by LC-ESI-MS/MS and MALDI-TOF mass spectrometry. *Chem. Res. Toxicol.*, **16**, 757–767.
35. Clauser,K.R. *et al.* (1999) Role of accurate mass measurement (+/- 10 ppm) in protein identification strategies employing MS or MS/MS and database searching. *Anal Chem*, **71**, 2871–2882.
36. Shen,J. and Fischer,S.M. (2010) Molecular profiling of the epidermis: a proteomics approach. Methods Mol. Biol., 585, 225–252
37. Kiguchi,K. *et al.* (2001) Constitutive expression of ErbB-2 in gallbladder epithelium results in development of adenocarcinoma. *Cancer Res*., **61**, 6971–6976.
38. Grivennikov,S.I. *et al.* (2009) Dangerous liaisons: STAT3 and NF-kappaB collaboration and crosstalk in cancer. *Cytokine Growth Factor Rev*., **21**, 11–19.
39. Acosta,J.C. *et al.* (2009) A role for CXCR2 in senescence, but what about in cancer? *Cancer Res*., **69**, 2167–2170.
40. Richmond,A. (2002) Nf-kappa B, chemokine gene transcription and tumour growth. *Nat. Rev. Immunol.*, **2**, 664–674.
41. Chun,K.S. *et al.* (2003) Curcumin inhibits phorbol ester-induced expression of cyclooxygenase-2 in mouse skin through suppression of extracellular signal-regulated kinase activity and NF-kappaB activation. *Carcinogenesis*, **24**, 1515–1524.
42. Lee,J.C. *et al.* (2007) Humulone inhibits phorbol ester-induced COX-2 expression in mouse skin by blocking activation of NF-kappaB and AP-1: IkappaB kinase and c-Jun-N-terminal kinase as respective potential upstream targets. *Carcinogenesis*, **28**, 1491–1498.
43. Surh,Y.J. *et al.* (2001) Molecular mechanisms underlying chemopreventive activities of anti-inflammatory phytochemicals: down-regulation of COX-2 and iNOS through suppression of NF-kappa B activation. *Mutat. Res.*, 480–481, 243–268.
44. Kundu,J.K. *et al.* (2007) Epigallocatechin gallate inhibits phorbol ester-induced activation of NF-kappa B and CREB in mouse skin: role of p38 MAPK. *Ann. NY. Acad. Sci.*, **1095**, 504–512.
45. Heizmann,C.W. *et al.* (2002) S100 proteins: structure, functions and pathology. *Front Biosci*., **7**, d1356–d1368.
46. Eckert,R.L. *et al.* (2004) S100 proteins in the epidermis. *J. Invest. Dermatol.*, **123**, 23–33.
47. Rojas,A. *et al.* (2010) Fueling inflammation at tumor microenvironment: the role of multiligand/RAGE axis. *Carcinogenesis*, **31**, 334–341.
48. Gebhardt,C. *et al.* (2002) Calgranulins S100A8 and S100A9 are negatively regulated by glucocorticoids in a c-Fos-dependent manner and overexpressed throughout skin carcinogenesis. *Oncogene*, **21**, 4266–4276.
49. Gebhardt,C. *et al.* (2008) RAGE signaling sustains inflammation and promotes tumor development. *J. Exp. Med.*, **205**, 275–285.
50. Sisskin,E.E. *et al.* (1982) Correlation between sensitivity to tumor promotion and sustained epidermal hyperplasia of mice and rats treated with 12-O-tetra-decanoylphorbol-13-acetate. *Carcinogenesis*, **3**, 403–407.
51. Lewis,J.G. *et al.* (1987) Early inflammatory changes in the skin of SENCAR and C57BL/6 mice following exposure to 12-O-tetradecanoylphorbol-13-acetate. *Carcinogenesis*, **8**, 889–898.
52. Naito,M. *et al.* (1987) Comparison of the histological changes in the skin of DBA/2 and C57BL/6 mice following exposure to various promoting agents. *Carcinogenesis*, **8**, 1807–1815.
53. Naito,M. *et al.* (1988) Susceptibility to phorbol ester skin tumor promotion in (C57BL/6 x DBA/2) F1 mice is inherited as an incomplete dominant trait: evidence for multi-locus involvement. *Carcinogenesis*, **9**, 639–645.
54. Suganuma,M. *et al.* (1999) Essential role of tumor necrosis factor alpha (TNF-alpha) in tumor promotion as revealed by TNF-alpha-deficient mice. *Cancer Res*., **59**, 4516–4518.
55. Moore,R.J. *et al.* (1999) Mice deficient in tumor necrosis factor-alpha are resistant to skin carcinogenesis. *Nat. Med.*, **5**, 828–831.
56. O'Hayer,K.M. *et al.* (2009) ELR+ CXC chemokines and oncogenic Ras-mediated tumorigenesis. *Carcinogenesis*, **30**, 1841–1847.
57. Cataisson,C. *et al.* (2009) Inducible cutaneous inflammation reveals a protumorigenic role for keratinocyte CXCR2 in skin carcinogenesis. *Cancer Res.,* **69**, 319–328.
58. Quigley,D.A. *et al.* (2009) Genetic architecture of mouse skin inflammation and tumour susceptibility. *Nature*, **458**, 505–508.

Received June 19, 2012; revised June 14, 2012; accepted June 16, 2012